FAILURE ANALYSIS OF AN OUTDOOR INSTRUMENT HOUSING

Jeffrey A. Jansen, The Madison Group, Madison, Wisconsin

Abstract

Cracking occurred within the housing for a piece of weather monitoring instrumentation being used as part of field service trial. The cracking was observed within the bosses used to secure the housing section to the mounting hardware. The focus of this investigation was the determination of the nature and cause of the failure. The results obtained during the evaluation of the failed housing indicated that the cracking occurred through three separate mechanisms. Significant factors in the failure included aspects of design, manufacturing, and the service conditions. This paper will review the testing performed to characterize the failure modes and identify the causes of the cracking, while demonstrating the analytical procedures used in the investigation.

Background

The instrument housing failed while being used as part of an extended field service product evaluation. Specifically, the failed unit had been installed outdoors at a coastal location within the Southeastern United States. Periodic routine inspection had identified cracking within bosses associated with hardware used to mount the housing to the mating bracket. Previous limited laboratory lifetime assessment had been completed without an indication of problems or failure.

The housing had been injection molded from an unfilled, flame retardant, UV stabilized, weather resistant grade of polycarbonate / poly(acrylonitrile:styrene:acrylate) (PC+ASA). The material had a melt flow rate specification of 20 g/10 min. to 40 g/10 min. under the test conditions of 260 °C and 5 kg. The housing material was over-molded onto stainless steel profiled threaded inserts.

After molding, the individual housing sections were assembled with the internal electrical components. The completed assembly was subsequently connected onto a mating bracket with metal hardware including M6 screws fastened into the over-molded stainless steel inserts. The screws are coated with Loctite® 243 adhesive. Nylon inserts were used on both sides of the bracket, and the bracket was secured to a mounting pole. Coaxial cable was then attached and vulcanizing tape applied.

In addition to the failed housing, an as-molded housing, which had never been in service or tested, was also received for comparison purposes. A typical sample of the molding resin was also submitted as a reference. Further, typical mounting hardware was also obtained.

Experimental

The failed and control parts were initially examined using a Keyence digital microscope at magnification between 5X and 200X.

Fracture surfaces from the cracked components were examined using a Tescan Vega3 scanning electron microscope (SEM). The specimens were cleaned ultrasonically in an aqueous solution of a mild detergent. Prior to the inspection, the surfaces were gold sputter coated to enhance the imaging.

Elemental analysis of various surfaces on the cracked housing was conducted in conjunction with the SEM examination on non-gold coated samples. The testing was performed using a Bruker system.

Samples representing the failed and reference parts were analyzed using Fourier transform infrared spectroscopy (FTIR) in the attenuated total reflectance (ATR) mode. A Nicolet iS5 spectrometer was used for the analysis.

Materials representing the parts were evaluated using differential scanning calorimetry (DSC). The testing was conducted using a TA Instruments Discovery 2500 DSC. The analysis involved heating the samples to an elevated temperature, followed by controlled cooling, and then reheating. A heating rate of 10 °C/min rate was utilized when maintaining the sample under a nitrogen atmosphere.

Specimens from the failed and reference sample materials were analyzed using thermogravimetric analysis (TGA). The testing was performed on a TA Instruments Discovery 5500 TGA system. The thermal program involved dynamic heating at 20 °C/min using sequential nitrogen and air purge atmospheres.

The average molecular weights of the part materials were indirectly evaluated by melt flow rate. The tests were performed in accordance with ASTM D 1238 using a temperature of 260 °C and a load of 5.0 kg. Moisture determinations made prior to testing were conducted through Karl Fischer titration.

Tests and Results

Fractographic Examination

Examination of the failed housing confirmed the presence of cracking within several of the bosses corresponding to the threaded metal inserts used to secure the housing to the mounting hardware. The cracked bosses exhibited multiple individual parallel longitudinal fractures (Figure 1). The cracks appeared to be primarily toward the upper mounting surface of the boss. Significantly, the appearance of the cracking was very consistent across the various bosses.

The cracking within the bosses lacked features associated with significant macro ductility, as would be apparent in the form of stress whitening or permanent deformation. Conversely, the cracks exhibited characteristics of brittle fracture from the exterior examination. The cracked bosses displayed significant localized discoloration. Specifically, the mounting surface as well as the areas surrounding the cracks exhibited an orange-brown coloration.

Some of the cracks were coincident with a distinct knit line in the boss wall (Figure 2). However, given the presence of multiple individual cracks on each boss, the fractures were not exclusively associated with knit lines.

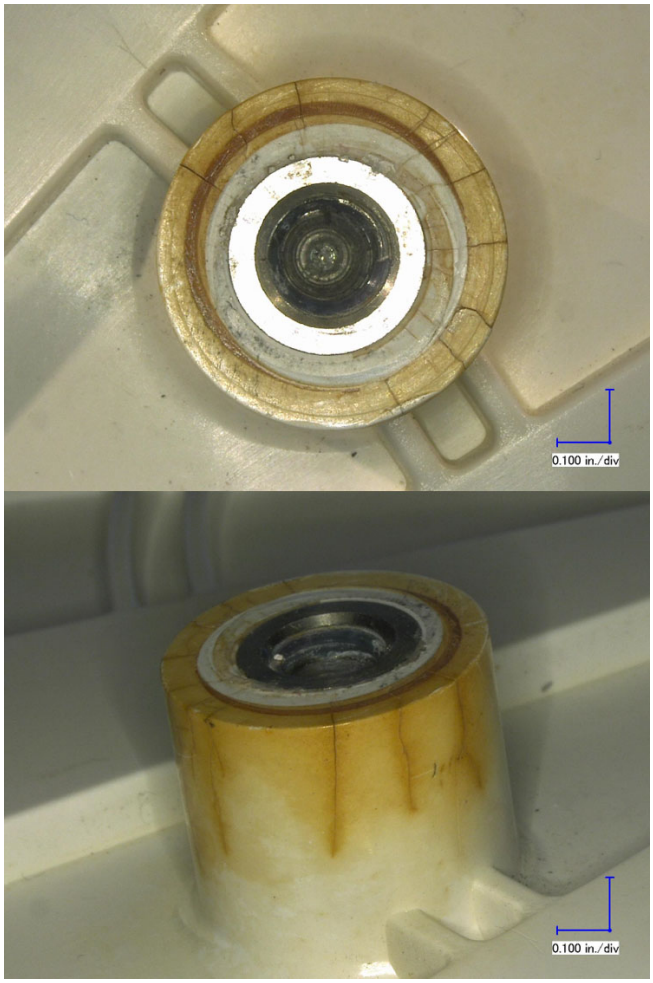

Figure 1. Photomicrographs showing typical cracking and discoloration within one of the housing bosses. No significant macro ductility is evident.

The microscopic examination of the mounting surface on several of the bosses showed a distinct circumferential band of discoloration. At higher magnification, it was apparent that this band corresponded to a zone of mud cracking on the surface of the boss (Figure 3). The form of the mud cracking was characteristic of localized molecular degradation of the boss material, resulting from contact with a deleterious chemical agent over a limited area. Further evidence of molecular degradation was apparent on the inner diameter of a number of the bosses toward the upper edge (Figure 4). Further, the inner diameter surface that corresponded to contact with the over-molded insert also showed the presence of a relatively high number of cracks. These cracks presented an irregular propagation pattern. In addition to the cracking, several of the bosses showed the presence of localized discoloration associated with adherent surface residue.

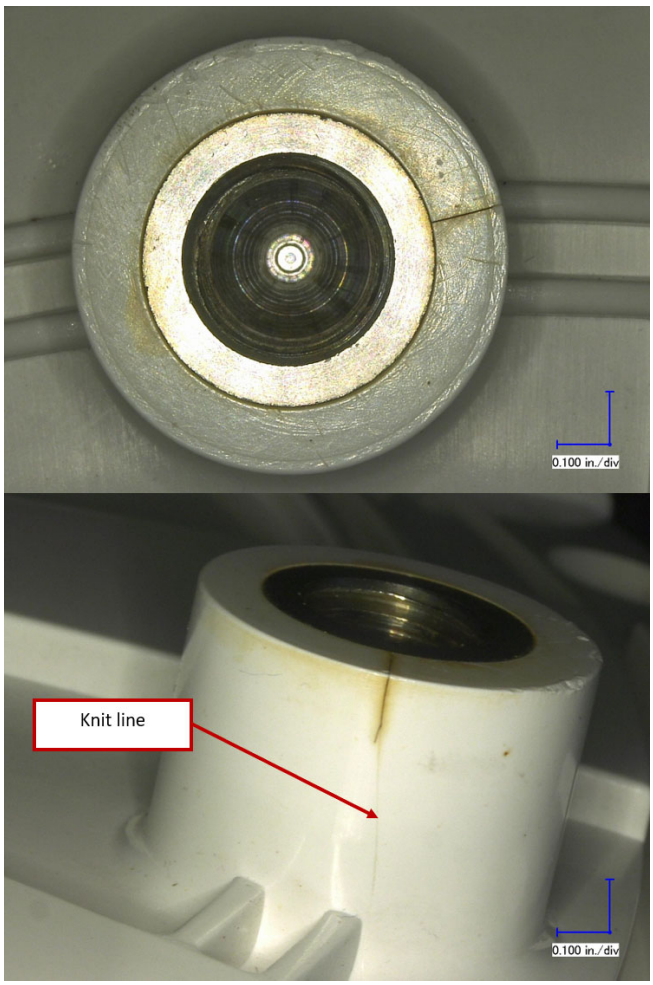

Figure 2. Photomicrographs showing cracking corresponding to the location of a knit line. No significant macro ductility is evident.

Microscopic examination of the exposed fracture surfaces revealed relatively good consistency across the various bosses. The inspection revealed localized areas of relatively smooth texture separated by course features. The observed features were indicative of the initiation and subsequent coalescence of multiple individual cracks, which produced the longitudinal fractures. The fracture surfaces lacked signs of significant macro ductility, instead presenting features characteristic of a brittle cracking mechanism. Some of the fracture surfaces exhibited the orange-brown discoloration noted during the exterior examination.

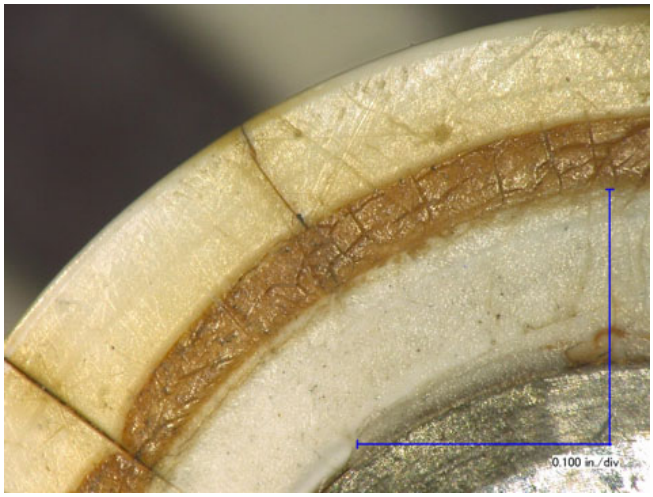

Figure 3. Photomicrograph showing localized discoloration. The discolored material displays substantial mud cracking associated with molecular degradation.

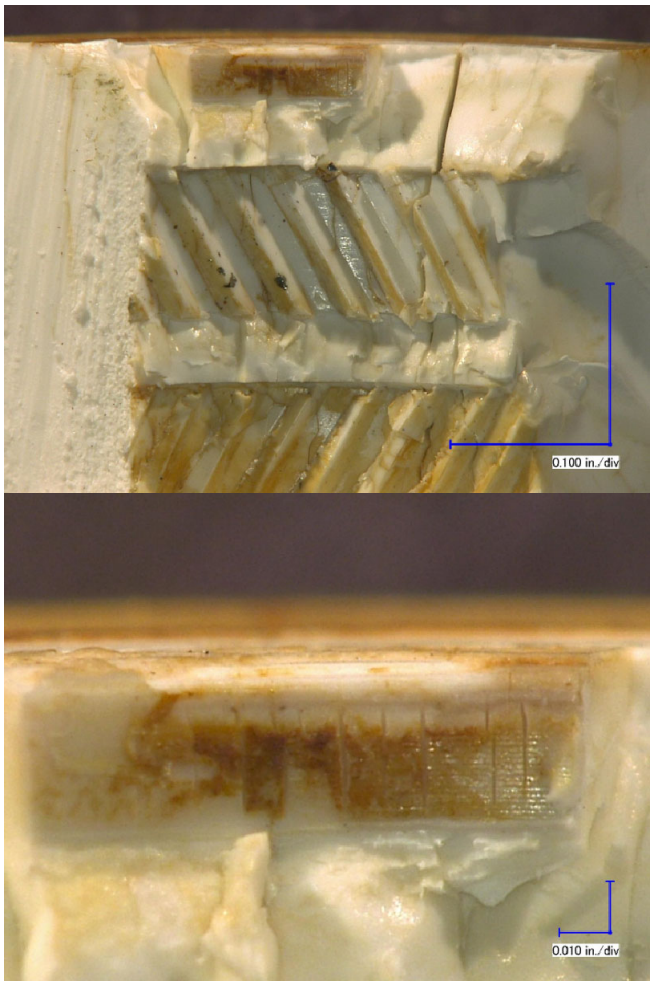

Figure 4. Photomicrographs showing features indicative of molecular degradation on the inner diameter of a typical boss.

The scanning electron microscopic (SEM) examination of the fracture surfaces from several of the bosses showed evidence of similarities, with some important distinctions (Figure 5). Inspection of the fracture surfaces from most of the bosses revealed two general locations of crack initiation. The larger and primary crack origins were positioned along the inner diameter of the boss wall, immediately adjacent to the molded-in metal insert (Figure 6). These crack origins were located within sharp corners of the insert. The sharp corners likely acted as points of significant stress concentration within the over-molded plastic. The crack origins exhibited a relatively smooth morphology, without signs of significant micro ductility, as would be apparent in the form of stretched fibrils or flaps. Further, the smooth origin morphology lacked features associated with rapid crack extension. After initiation, the cracking extended radially and subsequently longitudinally through the part wall.

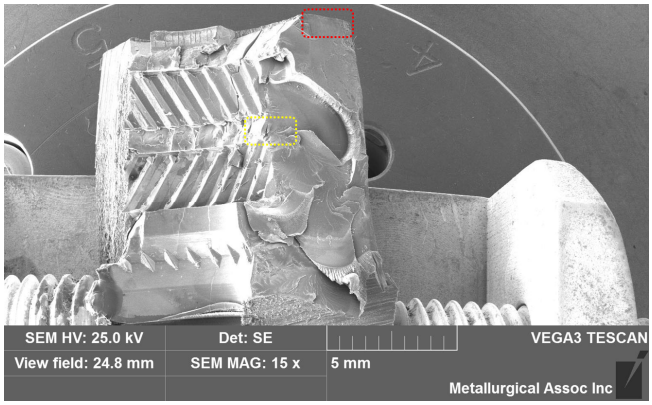

Figure 5. SEM image showing a typical boss fracture surface. Two distinct crack origin areas were identified.

The boss fracture surfaces also showed areas of crack initiation along the mounting surface (Figure 7). These origins also presented relatively smooth features consistent with brittle fracture through a slow crack initiation mechanism. Evidence of adherent debris was present within the crack origins. This debris was thought to correspond to the orange-brown coloration noted during the visual and microscopic examinations. After initiating, the cracking extended longitudinally down the wall of the boss.

Given the evidence of crack initiation along the mounting surface on a number of the bosses, and the associated discoloration, a representative mounting surface was examined via SEM. The SEM examination confirmed the presence of a localized band of mud cracking on the upper mounting surface. (Figures 8 and 9). The surface exhibited a characteristic pattern of mud cracking indicative of molecular degradation of the boss material. Additionally, signs of deposits on the surface were also present. The surface deposits were thought to correspond to the localized band of orange-brown coloration found during the visual and microscopic examinations.

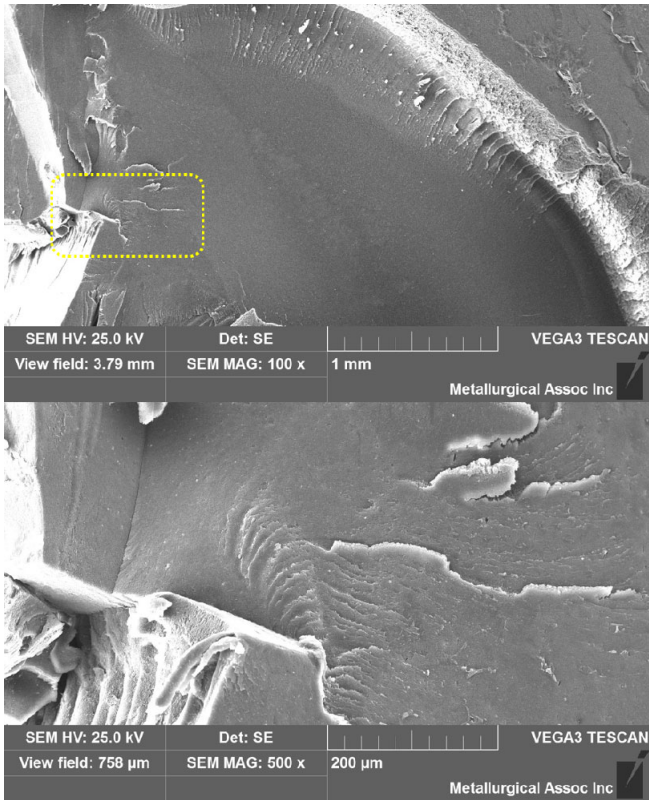

Figure 6. SEM images (yellow box in Figure 5) showing crack origin at a sharp corner corresponding to the metal insert. Brittle fracture features are present.

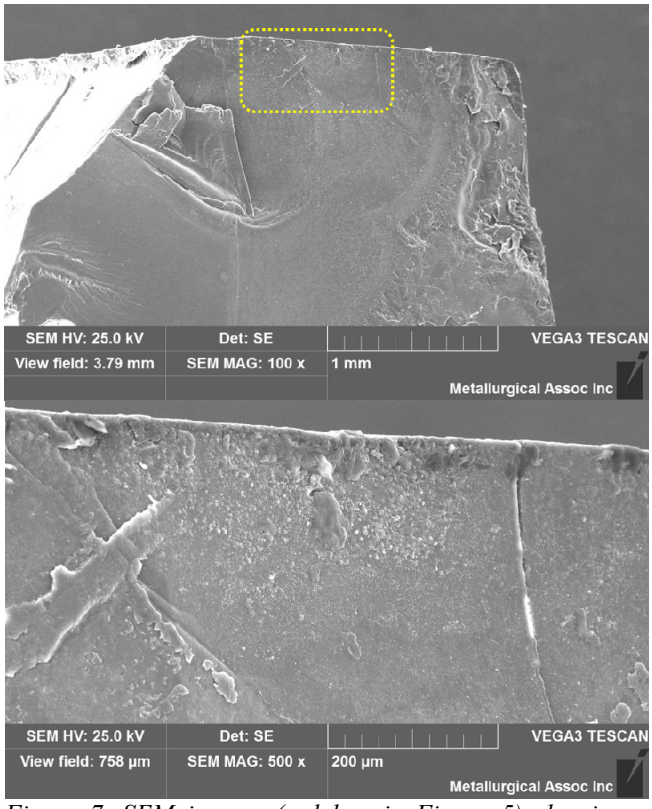

Figure 7. SEM images (red box in Figure 5) showing a crack origin along the mounting surface. Brittle crack features are present.

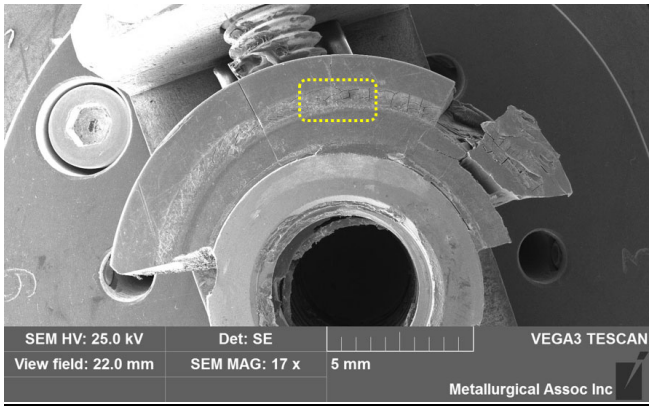

Figure 8. SEM image showing the mounting surface of a typical boss.

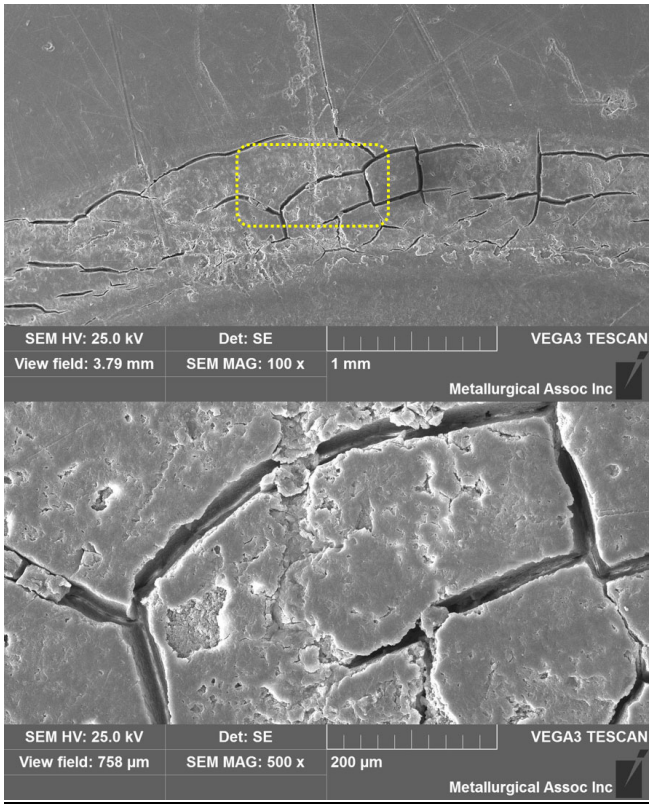

Figure 9. SEM images (yellow box in Figure 8) showing mud cracking associated with localized degradation of the housing material.

During the SEM examination of most of the boss fracture surfaces, some of the features were obscured by a relatively high concentration of nodular debris. This corresponded to the orange-brown residue observed during the microscopic examinations. At high magnification, the debris exhibited a mud-cracked appearance, consistent with the precipitation, drying, and embrittlement of a material that was once present as a liquid.

Remote to the crack origins, the fracture surface generally exhibited a noted increase in the level of micro ductility. This was accompanied by isolated features corresponding to

rapid crack extension, including hackle marks and river markings.

Some of the boss fracture surfaces also exhibited areas of crack initiation along the outer diameter of the boss wall. The fracture surface within the origin displayed a relatively smooth morphology, consistent with brittle fracture through slow crack initiation and growth. Some evidence of adherent residue was also present. Significantly, the outer diameter location of the crack origin and the pattern of crack propagation for these cracks, were consistent with the knit line observed on this boss surface during the microscopic examination.

An examination of the supplied as-molded housing revealed the presence of cracking within several of the bosses (Figure 10). A number of the bosses exhibited multiple individual parallel longitudinal cracks. The appearance of the cracking was very similar to that observed within the failed housing. As was the case with the failed housing, the cracking was primarily located toward the upper end of the boss. The external examination revealed features associated with brittle fracture, with no signs of significant macro ductility. Unlike the failed housing, no evidence of discoloration was apparent on the as-molded housing.

Microscopic inspection of the fracture surfaces revealed evidence indicating crack initiation along the inner diameter of the boss wall, proximal to the molded-in insert. The microscopic examination provided further evidence of brittle fracture, with no observed ductility.

The fracture surfaces from the as-molded housing were also examined via SEM. The fracture surfaces showed a single area of crack initiation positioned immediately adjacent to the molded-in metal insert (Figures 11 and 12). Specifically, the origin was located within a relatively sharp corner of the insert. The crack origin displayed an extremely smooth morphology. The observed features were indicative of a brittle fracture slow crack initiation and growth mechanism. Further, the features were relatively consistent with those observed on the corresponding origins in the failed housing bosses.

In order to understand the inherent mechanical response of the housing material, laboratory fractures were created through the failed housing material. Specimens were excised from the housing, with one subjected to slow bending loads representing mechanical overload, and the other loaded rapidly corresponding to impact. Both specimens were subsequently examined microscopically and with the SEM.

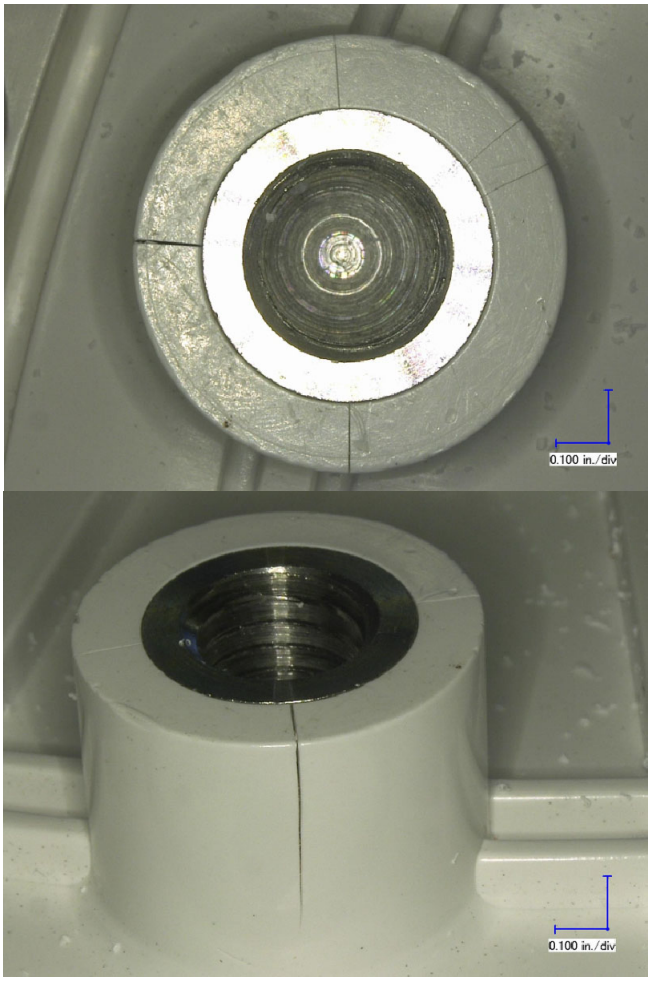

Figure 10. Photomicrographs showing cracking within one of the bosess on the submitted as-molded housing.

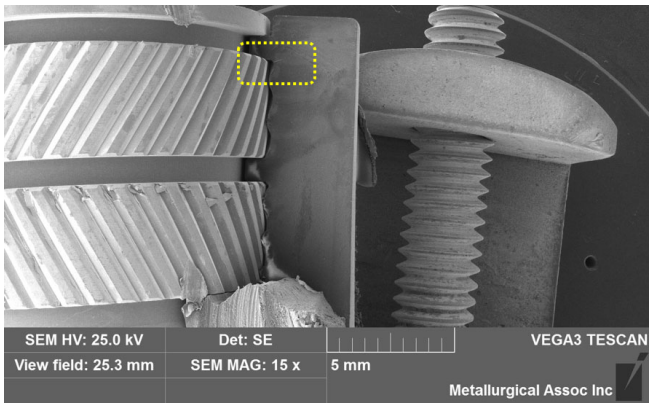

Figure 11. SEM images showing one of the boss fracture surfaces from the reference housing.

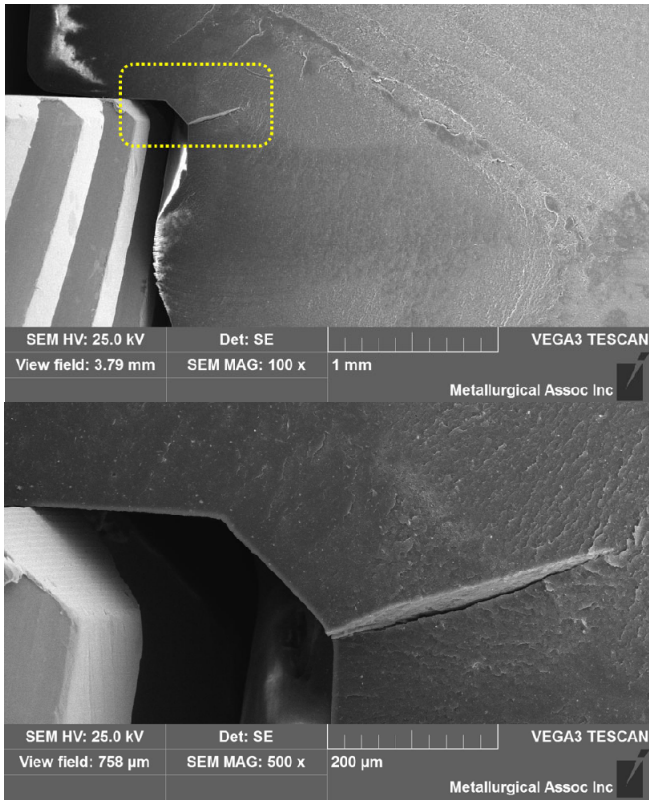

Figure 12. SEM images (yellow box in Figure 11) showing the crack origin location at a sharp corner corresponding to the metal insert. Brittle fracture features are present.

Examination of the overload specimen created through the application of slow bending stresses, showed a substantial level of macro and micro ductility. Visually, the sample showed a great degree of stress whitening and permanent deformation. Scanning electron images presented a relatively high concentration of stretched fibril formation (Figure 13). These fracture surfaces were in sharp contrast to those corresponding to the cracks within the failed and as-molded housings. Similar inspection of the impact specimen created through rapid loading showed minimal evidence of macro ductility. The specimen did not show evidence of significant stress whitening or permanent deformation. However, the SEM examination revealed a relatively high level of micro ductility. The SEM features were somewhat similar to the fracture surfaces remote to the crack origins on the failed and as-molded housings.

To further characterize the boss cracking, a cross-section was prepared through one of the bosses from the failed housing. A portion of the boss was excised, mounted in an epoxy medium, and polished to reveal the area of interest. The prepared cross-section revealed the extent of the relatively sharp corners created in the plastic by overmolding onto the metal insert (Figure 14). Such corners can act as points of severe stress concentration, thereby, multiplying any internal or external stress. Further examination of the cross-section revealed the presence of partial cracks extending out of the sharp corners. Some evidence of discoloration was apparent within and adjacent to the cracks. The cracking within the cross-section was consistent with the observations made during the fractographic examination of the failed and as-molded housing, indicating crack initiation along the inner diameter of the boss wall, immediately adjacent to the metal insert.

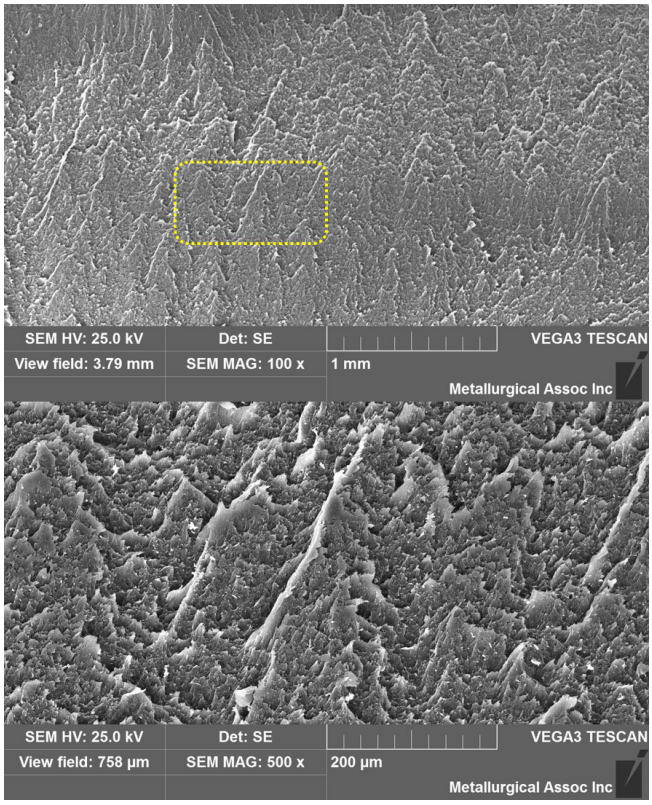

Figure 13. SEM images showing substantial micro ductility on the laboratory fracture surface.

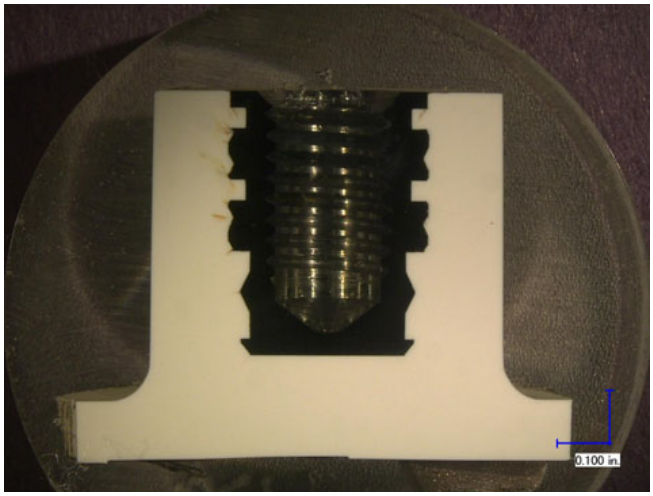

Figure 14. – Photomicrograph showing the cross-section prepared through a cracked boss on the failed housing. Cracking is apparent extending from sharp corners corresponding to the metal insert.

Fourier Transform Infrared Spectroscopy

Compositional analysis of the sample materials was performed using Fourier transform infrared spectroscopy (FTIR). Analysis of a specimen representing the submitted molding resin, produced results characteristic of a polycarbonate / poly(acrylonitrile:styrene:acrylate) (PC+ASA) resin blend (Figure 15). Further testing was performed on core specimens representing the failed housing and the as-molded housing. A direct comparison of the results yielded an excellent match, without apparent spectral differences. No evidence was found through the FTIR analysis to indicate the presence of bulk contamination or other anomalies within the molded housing materials.

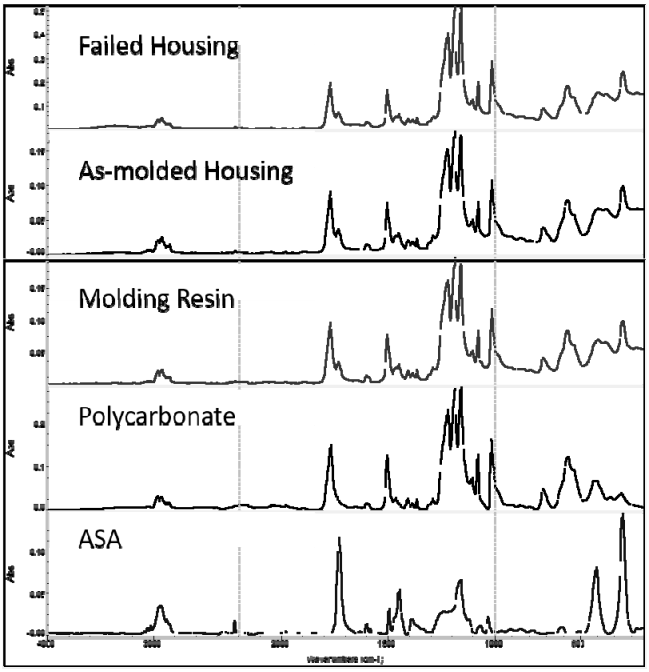

Figure 15. – FTIR spectra obtained on the housing samples.

Energy Dispersive X-ray Spectroscopy

Energy dispersive X-ray spectroscopy (EDS) was performed on the housing samples. Initially, materials representing the plastic housing were tested. The analysis of the molding resin showed relatively high concentrations of carbon and oxygen; moderate levels of bromine, titanium, and antimony; and trace amounts of silicon and sulfur. The carbon and oxygen were associated with the base polymer. The bromine and the antimony were thought to be present as flame retardant additives. The titanium was likely titanium dioxide. Analysis of a core sample representing the failed housing produced a very similar elemental profile.

An analysis was also conducted on the brown residue present on one of the boss fracture surfaces. Elements associated with the plastic resin were present. However, the residue sample contained a much higher level of oxygen relative to carbon, as compared to the resin and housing core materials. Additionally, the residue contained a relatively high concentration of iron, as well as significant levels of chromium and nickel. Importantly, the presence of chlorine was also identified. Accounting for the elements associated with the base plastic, the results obtained on the brown residue were consistent with corrosion products of a stainless steel component. Chlorine-based compounds are known to cause corrosion within stainless steel alloys.

Table 1
EDS Analysis Results – Plastic Housing
(Relative Weight Percent)

Element	Molding Resin	Failed Part - Core	Fracture Surface Deposit
Carbon	77.2	75.9	26.7
Oxygen	15.3	16.9	48.5
Titanium	1.5	2.1	0.8
Antimony	1.4	1.2	0.6
Bromine	4.4	3.5	1.2
Silicon	0.1	0.1	0.3
Sulfur	0.1	0.2	0.6
Chlorine	---	0.1	0.6
Sodium	---	0.1	---
Iron	---	---	18.1
Chromium	---	---	2.1
Nickel	---	---	0.7
Magnesium	---	---	0.1

Differential Scanning Calorimetry

Differential scanning calorimetry (DSC) of the molding resin and the failed housing material produced relatively similar DSC thermograms (Figure 16). A review of the second heating results showed that the molding resin underwent a dual shift in heat flow associated with two individual glass transitions within the material. Glass transition temperatures of 110 °C and 135 °C were obtained, representing the poly(acrylonitrile:styrene:acrylate) (ASA) and polycarbonate (PC) constituents, respectively. The presence of two distinct glass transitions indicated that the material is a resin blend having a two-phase morphology. A disturbance in the thermogram baseline was observed at approximately 300 °C representing partial material degradation, likely within the flame retardant package.

The second heating DSC thermogram representing the failed housing material also showed the dual glass transitions. While the glass transition associated with the ASA remained relatively consistent, the glass transition corresponding to the PC was somewhat lower, 132° C. This reduction in glass transition temperature was thought to represent variation in molecular structure between the molding resin and the failed housing material, within the polycarbonate domain. Considering the DSC results, it was evident that some molecular structural differences existed between the molding resin and the failed part material.

Thermogravimetric Analysis

Thermogravimetric analysis (TGA) of the resin and failed housing was performed to further evaluate the compositions of the material (Figure 17). Analysis of the two materials produced generally similar weight loss profiles. Under the dynamic nitrogen purge, the samples underwent a multi-stage weight loss, with combined losses of approximately 86%. These weight losses were associated with the initial

stages of thermal decomposition of the polymers. Further heating under an air atmosphere resulted in a weight loss of 11%, corresponding with the combustion of carbonaceous char formed during the initial thermal decomposition of the polymer. This pattern of weight loss was consistent with the expected results for a polycarbonate/ poly(acrylonitrile:styrene:acrylate) (PC+ASA) resin. Upon completion of the analysis, a non-combusted residue content of approximately 4% remained, indicating that the material was not formulated with a significant level of fillers.

While the two materials produced similar quantitative results, a direct comparison of the weight loss profiles revealed that the failed housing material underwent a weight loss at a significantly lower temperature. This variation in thermal decomposition was suggestive that the failed part material was less thermally stable. Specifically, the weight loss corresponding to the polycarbonate was shifted to a substantially lower temperature. This was also supported by a review of the localized maximum in the weight loss derivative curve. The molding resin showed the polycarbonate weight loss to be centered at 507 °C, while the temperature was reduced to 469 °C in the failed part material. The identification of molecular differences in the materials through TGA, was consistent with the results obtained during the DSC analysis. This type of variation is often associated with molecular degradation.

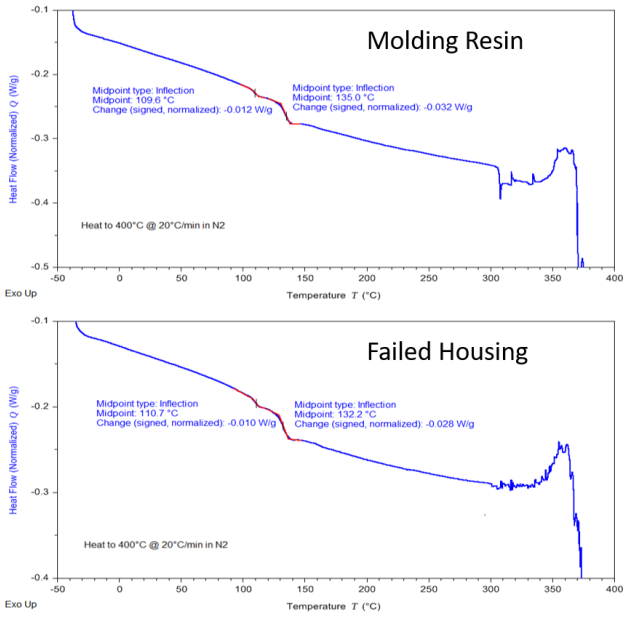

Figure 16. – The DSC thermograms obtained on the molding resin and the failed housing material.

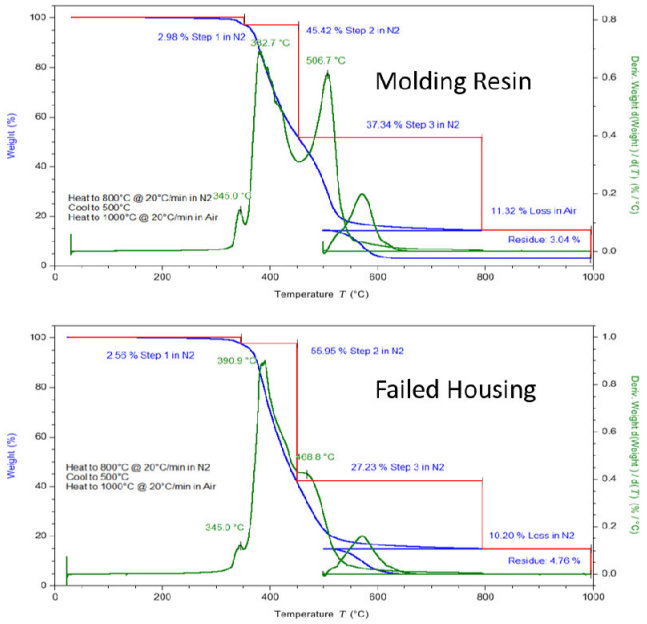

Figure 17. – The DSC thermograms obtained on the molding resin and the failed housing material.

Melt Flow Rate

Melt flow rate (MFR) testing of the supplied molding resin produced a melt flow rate of 45.8 g/10 min. This was substantially higher than the value indicated on the resin datasheet, a nominal value of 22 g/10 min. Additionally, the obtained value was higher than the specification range indicated on the certificate of analysis, 20 g/10 min. to 40 g/10 min. The reason for the disparity was not readily apparent.

The results obtained on the as-molded and failed housings were notably higher than that obtained on the molding resin, 102.8 g/10 min. and 75.9 g/10 min., respectively. This represented a significant reduction in average molecular weight compared with the molding resin. The results obtained on the two molded parts were indicative of severe and excessive molecular degradation of the housing material.

Table 2
Melt Flow Rate Test Results
(g/10 min.)

Test	Molding Resin	As-Molded Housing	Failed Housing
1	46.9	104.0	75.2
2	44.9	101.3	73.1
3	44.8	103.0	77.2
4	45.1	---	78.1
5	46.1	---	---
6	47.1	---	---
Average	45.8	102.8	75.9

Conclusion

It was the conclusion of the investigation that the cracking within the housing bosses occurred through three different brittle fracture via slow crack initiation and propagation mechanisms. The most prevalent cracking was associated with interference stresses between the molded-in metal inserts and the over-molded bosses. The failures occurred through creep rupture, a brittle fracture, slow crack growth mechanism. Creep rupture occurs via the exertion of stress over a period of time that exceeds the long-term strength of the material. This stress is most often well below the yield point of the material. Oftentimes, such stress occurs within plastic molded over metal inserts as a result of the differential in coefficient of thermal contraction between the plastic and the metal. The over-molded plastic shrinks to a much greater degree than the metal insert during cooling as part of and after injection molding, producing interference stress.

Additional cracking within the bosses resulted from the presence of poorly fused knit lines. Knit lines are produced through the union of two flow fronts extending around design features, such as the boss, during the injection molding process. Knit lines can represent localized areas of reduced mechanical integrity if the molecules at the flow fronts are not adequately entangled upon solidification. The knit line failures also occurred through creep rupture.

The knit line cracking initiated along the outer diameter of the boss wall, likely the weakest area on the boss because of locally poor fusion. It is significant to note that because many of the bosses exhibited multiple cracks, the fractures were not exclusively associated with knit lines.

The third type of cracking present on the housing bosses occurred through localized molecular degradation of the plastic along the upper mounting surface of the boss. A circumferential ring was present on the mounting surface of many of the bosses that displayed an orange-brown discoloration, and during microscopic examination presented distinctive mud cracking. Localized molecular degradation resulted from chemical attack of the molded plastic resin. The form of the cracking was indicative of a chemical reaction that resulted in significant molecular weight reduction of the polymer. The reduction in molecular weight produced a decline in the plastic material properties, including short-term and long-term mechanical strength. The cracking initiated within the zone of localized molecular degradation, and extended longitudinally through the boss wall.

Based upon analysis, the chemical agent thought to be responsible for the molecular degradation was identified as ferrous chloride. Ferrous chloride is produced as a corrosion product of ferrous alloys, including stainless steel. A significant level of chlorine was identified within the orange-brown debris present on, and adjacent to, the fracture surfaces. Chlorine-based compounds are known to produce corrosion in stainless steel alloys. Given the configuration, the most likely mechanism is crevice corrosion. However, further evaluation would be required to confirm this.

The observations made during the fractographic evaluation of the failed and as-molded housings were not consistent with overload or impact failures created during a relatively short period of time. Further, no signs of chemical interaction, such as environmental stress cracking (ESC) were apparent.

Melt flow rate testing of the failed housing and as-molded housing materials produced results indicating severe molecular degradation, associated with the injection molding process. Molecular degradation represents the reduction in molecular weight of the polymer, and reduces the mechanical integrity of the molded part, rendering the part susceptible to premature failure. This molecular degradation is thought to be a primary factor in the cracking of the housing bosses. Results obtained during differential scanning calorimetry and thermogravimetric analysis supported the conclusion that the housing materials had been substantially degraded. In particular, the thermogravimetric analysis indicated that the degradation was most likely associated with the polycarbonate phase of the resin blend.

Keywords

failure analysis, molecular degradation, creep, PC+ASA